TIME-DOMAIN SIMULATION OF FUNCTIONS AND DYNAMICAL SYSTEMS OF BESSEL TYPE

K. Trabelsi[†,*], **T. Hélie**[‡,*], **D. Matignon**[†,*]
[†]GET Télécom Paris, TSI dept. & CNRS UMR 5141. 37-39 rue Dareau, 75014 Paris, France
[‡]Ircam, Centre Pompidou, Analysis/Synthesis team & CNRS UMR 9912. 1 place Stravinsky, 75004 Paris, France.
[*]Email: karim.trabelsi@enst.fr, thomas.helie@ircam.fr, denis.matignon@enst.fr
[*] Work supported by the CONSONNES project, ANR-05-BLAN-0097-01.

Abstract

Two methods are investigated for the time-domain simulation of functions and dynamical systems of Bessel type, involved in wave propagation (see *e.g.* [1], [8], [2]). Both are based on complex analysis and lead to finite-dimensional approximations. The first method relies on optimized parametric contours and provides asymptotic convergence rates. The second is based on cuts and integral representations, whose approximations prove efficient, even at low orders, using ad hoc frequency criteria.

1 Model under study

For $\Re\mathrm{e}(s) > -\varepsilon$, let $\widehat{J^\varepsilon}(s) = [(s+\varepsilon)^2+1]^{-1/2}$ be the Laplace transform of $J^\varepsilon(t) = \mathrm{e}^{-\varepsilon t} J_0(t)$ for $t \geq 0$ (cf. [3]). The general formula can be derived:

$$J^\varepsilon(t) = \frac{1}{2i\pi}\int_{\mathbb{R}} \mathrm{e}^{\gamma(u)\,t}\widehat{J^\varepsilon}(\gamma(u))\,\gamma'(u)\,\mathrm{d}u, \qquad (1)$$

where the $\mathcal{C}^1$ parametrization $u \mapsto \gamma(u)$ defines a curve $\mathcal{C}$ which encloses all the singularities of $\widehat{J^\varepsilon}$: poles, branching points and cuts. In the case $\gamma(u) = \sigma + 2i\pi u$ for $\sigma > 0$, we recover the standard Bromwich formula.

2 Optimized parametrized Bromwich contours

In this section, we approximate $J^\varepsilon(t)$ on an interval $[t_0, t_1]$ following Talbot's approach, [11]. More precisely, we use two parametrized Bromwich contours proposed in [12], either the parabola $\gamma(u) = \mu(iu+1)^2 + \beta$, or the hyperbola $\gamma(u) = \mu(1+\sin(iu-\alpha)) + \beta$ where $u \in]-\infty, \infty[$, $\mu > 0$ regulates the width of the contours, β determines their foci, and α defines the hyperbola's asymptotic angle. The motivation for these choices is their simplicity and suitability for a trapezoidal approximation of (1) by:

$$J^\varepsilon_{h,N}(t) = \frac{h}{2i\pi}\sum_{n=-N}^{N} \mathrm{e}^{\gamma(nh)t}\widehat{J^\varepsilon}(\gamma(nh))\,\gamma'(nh). \qquad (2)$$

Indeed, one can assess the discretization errors by classical techniques (see [7], [10, § 3.2]) to obtain, for all $t \geq 0$,

$$|J^\varepsilon(t) - J^\varepsilon_{h,\infty}(t)| \leq E_d^-(t) + E_d^+(t) \text{ with } E_d^\pm = \frac{M^\pm(t)}{\mathrm{e}^{2\pi c^\pm/h}-1},$$

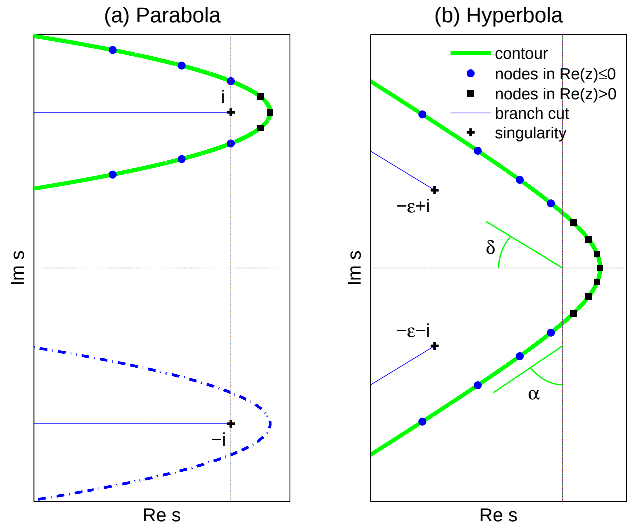

Figure 1: Parametrized Bromwich contours. (a) left: parabolas; (b) right: hyperbola.

owing to the holomorphic extension of the integrand in (1) to $\mathcal{U} = \{u \in \mathbb{C} : -c^- < \Im(u) < c^+\}$ (see [12, Th. 2.1]). For a given (t_0, t_1, N), the parameters μ, h and a range $]\alpha^-, \alpha^+[$ for α are derived in [12, § 3, 4] by asymptotically balancing the discretization errors $E_d^\pm$, and the truncation error E_t which is assumed to behave like the magnitude of the last term in (2), that is, $\mathcal{O}(|h\mathrm{e}^{\gamma(Nh)t}\widehat{J^\varepsilon}(\gamma(Nh))\gamma'(Nh)|)$. Parameter β is assumed to have a small real part.

2.1 *An optimized parabolic contour*

One way to simulate the Bessel function J^ε is to consider it as the *convolution* of the two functions $j^\varepsilon_\pm(t) = \mathcal{L}^{-1}[1/\sqrt{s+\varepsilon\mp i}] = (\pi t)^{-1/2}\mathrm{e}^{(\pm i-\varepsilon)t}$. The function j^ε_+ can be represented using a parabolic contour adapted to the cut $i - \varepsilon + \mathbb{R}^-$ (j^ε_- is straightforwardly inferred by hermitian symmetry, see Fig. 1a). However, two problems arise: first, the theoretical L^∞-error (see [12, §4])

$$E_N \triangleq \sup_{t\in[t_0,t_1]} |j^\varepsilon_\pm(t) - j^\varepsilon_{\pm,h,N}| = \mathcal{O}(\mathrm{e}^{-2\pi N/\sqrt{8\Lambda+1}}), \quad (3)$$

where $\Lambda = t_1/t_0$, is not matched numerically. Nevertheless, this relation is recovered by taking $t'_0 = 4\,t_0$, as observed in Fig. 2 (a possible reason could be the singularity of $j_{\pm}^{\varepsilon}$ at $t = 0^+$). Second, numerical convolution fails for

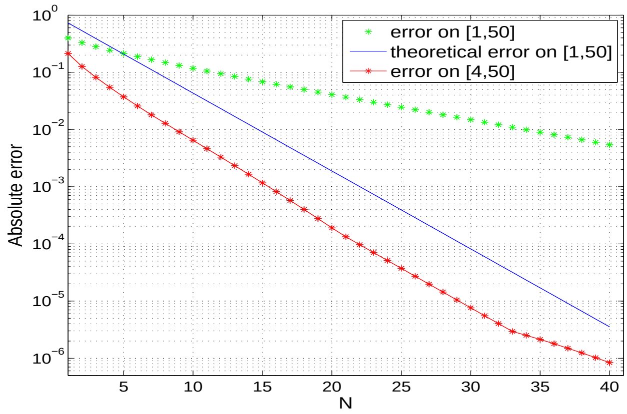

Figure 2: Approximation of $j_{\pm}^{0}$ for $(t_0, t_1) = (1, 50)$. Theoretical (-) and numerical (.,*) errors.

lack of information on the interval $[0, t_0[$ and badly approximated values on $[t_0, t_0']$. Using hyperbolic contours for J^{ε} will help cope with both these problems, due to the decomposition into *singular* functions $j_{\pm}^{\varepsilon}$.

2.2 An optimized hyperbolic contour

Here, we adopt the hyperbolic contour Fig. 1b, which is appropriate for our model problem, since the singularities lie in a *sectorial* region. In this case, the optimal convergence rate is:

$$E_N = \mathcal{O}(\mathrm{e}^{-B(\alpha,\Lambda)N}), \quad \alpha \in]\pi/4 - \delta/2, \pi/2 - \delta[, \quad (4)$$

where δ defines the sector the singularities lie in (see Fig. 1b) and B behaves like $(1/\ln\Lambda)$ for large Λ (see [12, § 4]). Further numerical simulations show that optimizing B w.r.t. α divides the rate by 10 at most, compared to the choice: $\alpha = \pi/4 - \delta/2 + 0$.

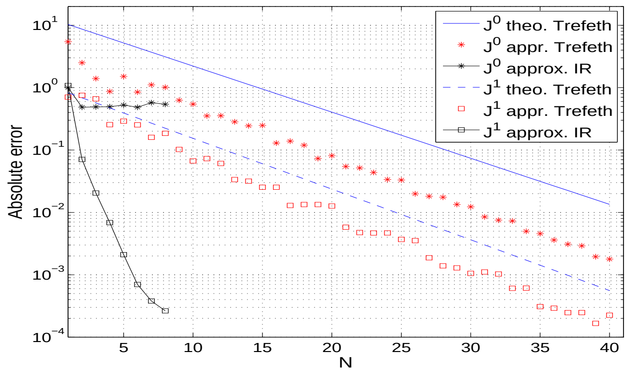

Figure 3: Approximation of $J_0(t)$ for $t \in [1, 5]$, and of $J^1(t)$ for $t \in [0.1, 50]$. Theoretical and numerical errors.

Figure 3 shows that the greater ε, the better the approximation: as ε gets smaller, the asymptotic sector widens; therefore, to yield comparable convergence rates in (4), one needs to take $\Lambda^{\varepsilon=1} = 100\,\Lambda^{\varepsilon=0}$. For $\varepsilon = 1$, β is zero, while for $\varepsilon = 0$, β has to be tuned heuristically, with a small real part (here, $\beta = 0.25$).

Improvements brought by hyperbolic over parabolic contours are yet unsufficient: a lingering problem is due to the nodes with a *positive* real part, which prevent simulation for $t \geq t_1$ (exponential divergence). This is tackled by the exact and approximated integral representations.

3 Optimal integral representations

The transfer function $\widehat{J^{\varepsilon}}(s)$ is analytic in the Laplace domain $\Re\mathrm{e}(s) > -\varepsilon$. In this section, we consider analytic continuations $\widehat{J_{\theta}^{\varepsilon}}$ of $\widehat{J^{\varepsilon}}$ over $\mathbb{C} \setminus (\mathcal{C}_{\theta} \cup \overline{\mathcal{C}_{\theta}})$, with the cuts $\mathcal{C}_{\theta} = \left(i - \varepsilon + \mathrm{e}^{i\theta}\mathbb{R}^+\right)$ and $\overline{\mathcal{C}_{\theta}}$, and $\widehat{J_{\theta}^{\varepsilon}}$ defined by:

$$\begin{aligned} \widehat{J_{\theta}^{\varepsilon}}(s) &= \frac{1}{\sqrt[(\theta)]{s + \varepsilon - i}\;\sqrt[(2\pi-\theta)]{s + \varepsilon + i}}, \qquad (5) \\ \sqrt[(\theta)]{\rho\,\mathrm{e}^{i\phi}} &= \sqrt{\rho}\,\mathrm{e}^{i\phi/2}, \text{ if } \rho \geq 0,\ \phi \in]\theta - 2\pi, \theta[. \end{aligned}$$

3.1 Principle

For $u \geq 0$, let $\gamma_u = i - \varepsilon + \mathrm{e}^{i\theta}u$ be a parametrization of $\mathcal{C}_{\theta}$. Function $\widehat{J_{\theta}^{\varepsilon}}(s)$ has hermitian symmetric decomposition $\left(\widehat{J_{\theta}^{\varepsilon+}}(s) + \overline{\widehat{J_{\theta}^{\varepsilon+}}(\overline{s})}\right)/2$, with integral representation:

$$\begin{aligned} \widehat{J_{\theta}^{\varepsilon+}}(s) &= \int_{\mathcal{C}_{\theta}} \frac{\mu_{\theta}(\gamma)}{s - \gamma}\,\mathrm{d}\gamma = \int_{\mathbb{R}^+} \frac{\mu_{\theta}(\gamma(u))}{s - \gamma(u)}\gamma'(u)\,\mathrm{d}u, \\ \mu_{\theta}(\gamma_u) &= \lim_{\eta \to 0^+} \frac{H_{\theta}(\gamma_u + i\gamma_u'\eta) - H_{\theta}(\gamma_u - i\gamma_u'\eta)}{2i\pi} \\ &= \left[\pi\sqrt{u}\;\sqrt[(\theta)]{2i + \mathrm{e}^{i\theta}u}\right]^{-1} \mathrm{e}^{i\frac{\pi - \theta}{2}} \qquad (6) \end{aligned}$$

which fulfills the well-posedness criterion (see e.g. [6]):

$$\int_{\mathcal{C}_{\theta}} \left| \frac{\mu(\gamma)\,\mathrm{d}\gamma}{1 - \gamma} \right| \triangleq \int_{\mathbb{R}^+} \left| \frac{\mu(\gamma_u)}{1 - \gamma_u}\gamma_u' \right| \mathrm{d}u < \infty.$$

These systems are approximated by the finite-dimensional models:

$$\widetilde{H}_{\mu}(s) = \frac{1}{2}\sum_{k=0}^{K}\left[\frac{\mu_k}{s - \gamma_k} + \frac{\overline{\mu_k}}{s - \overline{\gamma_k}}\right], \qquad (7)$$

where γ_k are a finite set of poles located on the cut $\mathcal{C}_{\theta}$. For a given location (so far, only a *heuristic* approach based on Bode diagrams is being used), the weights μ_k are optimized for the weighted least-squares criterion:

$$\mathcal{C}(\mu) \triangleq \int_{\mathbb{R}^+} \left| \widetilde{H}_{\mu}(2i\pi f) - \widehat{J^{\varepsilon}}(2i\pi f) \right|^2 w(f)\,\mathrm{d}f, \quad (8)$$

with the weight $w(f) = 1_{[f^-,f^+]}(f)/(f\,|\widehat{J^\varepsilon}(2i\pi f)|^2)$. The latter takes into account a bounded frequency range, a logarithmic frequency scale, and a relative error measurement (see [6] for details). Note that the Laplace transform of (2) is of the form (7) with $\gamma_k = \gamma(kh)$ and $\mu_k = 2h\,\gamma'(kh)\,\widehat{J^\varepsilon}\big(\gamma(kh)\big)$ for $0 \le k \le K = N$.

3.2 Numerical results

We consider four cases: **(C1)** J^0 with $\theta = \pi$, **(C2)** J^1 with $\theta = \pi$, **(C3)** J^0 with $\theta = \frac{\pi}{2}$, **(C4)** J^1 with $\theta = \alpha + \frac{\pi}{2}$. Results are presented on Fig. 4 for poles ($1 \le K \le 8$) on $\mathcal{C}_\theta$ with log-spaced u from $u_{min} = 5.10^{-4}$ to $u_{max} = 5.10^3$.

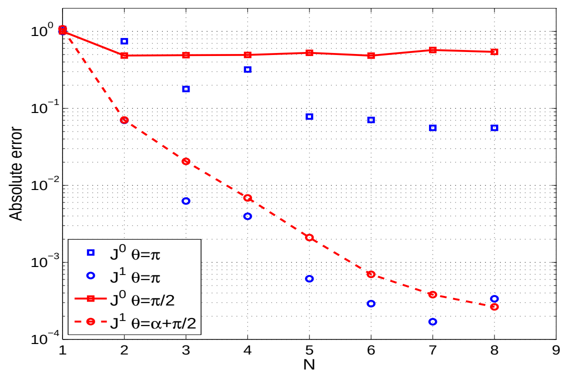

Figure 4: Approximations of J^0 and J^1 for various cuts ($\theta \approx \frac{\pi}{2}$ and $\theta = \pi$). Numerical errors.

Comparisons are also displayed in Fig. 3 for **(C3)** and **(C4)**. Note that horizontal cuts (i.e. $\theta = \pi$) improve the approximations significantly.

Conclusion and Perspectives

The first method seems appealing because of the a priori convergence rate, but this is only asymptotic. Other drawbacks are: sensitivity of the parameters of the contours, and existence of unstable nodes preventing long-range time simulation. On the contrary, the second method gives stable approximate systems, and the criterion used to build them is very flexible, user-designed; still, no theoretical convergence rate seems to be available, but low-order results can be very good.

Both these methods need to be tested on a wider family of transfer functions (see [3, chap. 4]). The role of the parameters in the first method has to be investigated more thoroughly and systematically. Another direction of research to be pursued in the near future is to compare our results with other techniques, based on Gauss-Legendre quadature points in the evaluation of the integral representation, which also have some very useful a priori error estimates, see e.g. [4].

References

[1] J. Audounet, D. Matignon, and G. Montseny. Perfectly absorbing boundary feedback control for wave equations: a diffusive formulation. In 5th *Waves conf.*, p. 1025–1029, Santiago de Compostela, Spain, July 2000. INRIA, SIAM.

[2] M. Duran, I. Muga, and J.-C. Nédélec. The Helmholtz equation in a locally perturbed half-plane with passive boundary. *IMA J. Appl. Math.*, 71 (2006), no. 6, 853–876.

[3] D. G. Duffy. *Transform methods for solving partial differential equations*. CRC Press, 1994.

[4] L. Greengard and P. Lin. Spectral approximation of the free-space heat kernel. *Appl. Comput. Harmonic Anal.*, 9(83), 2000.

[5] Th. Hélie and D. Matignon. Numerical simulation of acoustic waveguides for Webster-Lokshin model using diffusive representations. In 6th *Waves conf.*, p. 72–77, Jyväskylä, Finland, July 2003. INRIA.

[6] Th. Helie and D. Matignon. Representations with poles and cuts for the time-domain simulation of fractional systems and irrational transfer functions. *Signal Processing*, 86:2516–2528, jul 2006.

[7] P. Henrici. *Applied and computational complex analysis*, vol. 2. Wiley Interscience, 1977.

[8] D. Levadoux and G. Montseny. Diffusive realization of the impedance operator on circular boundary for 2D wave equation. In 6th *Waves conf.*, p. 136–141, Jyväskylä, Finland, July 2003. INRIA.

[9] D. Matignon. Stability properties for generalized fractional differential systems. *ESAIM: Proceedings*, 5:145–158, December 1998.

[10] F. Stenger. Numerical methods based on Whittaker cardinal, or sinc functions. *SIAM Rev.*, 23(2):165–224, 1981.

[11] A. Talbot. The accurate numerical inversion of Laplace transforms. *J. Inst. Math. Appl.*, 23(1):97–120, 1979.

[12] J. A. C Weideman and L. N. Trefethen. Parabolic and hyperbolic contours for computing the Bromwich integral. *Math. Comput.*, 2007. to appear.